Power System Technology
Volume 50, No. 2, 2026
ISSN: 1000-3673

Hybrid PID-Neural Network Control Strategy for Load Frequency Control in Smart Power Systems

Uchegbu Chinenye Eberchi
Department of Electrical and Electronic Engineering, Abia State University Uturu
Ezekiel Nnamere Aneke
Department of Electrical and Electronic Engineering, Abia State University Uturu
Inyama Kelechi
Department of Electrical and Electronic Engineering, Abia State University Uturu
Nwaogu Christopher
Department of Electrical and Electronic Engineering, Abia State University Uturu
Ahuchaogu Nnamdi
Department of Electrical and Electronic Engineering, Abia State University Uturu
Mama Rotenna Ovid
Department of Computer Engineering Veritas University Abuja
Ikwunze Okechukwu
Department of Electrical and Electronic Engineering Abia State Polytechnic Aba
Ogbodo Ikechukwu Ogbodo
State University of Medical and Applied Science, Enugu

Abstract

Load frequency control remains one of the most pressing operational challenges in modern smart power systems, particularly as intermittent renewable energy sources displace conventional synchronous generators and erode system inertia. Conventional proportional-integral-derivative controllers, long relied upon for frequency regulation, exhibit performance degradation under nonlinear, time-varying conditions that characterise contemporary grid operations. In this paper, a hybrid control strategy is proposed by combining proportional-integral-derivative controller with a feedforward neural network to implement load frequency control for two-area interconnected power system. The proportional-integral-derivative term corrects the steady-state error and the base frequency response; while the neural network provides an adaptive corrective signal that reduces residual transient error and improves frequency recovery under stochastic and time-varying load perturbations within the linearised plant framework. The neural network is then trained offline with the Levenberg-Marquardt backpropagation via simulated area control error trajectories, and it subsequently runs online without any retraining of its weights. Simulation experiments on a two-area thermal power system (TAPS) show that for step load perturbations, stochastic load variations and renewable energy penetration, the proposed strategy reduces the integral squared error by 78% and the integral time absolute error by 77.4% compared to a classical proportional-integral-derivative controller. Peak frequency deviation is curtailed from 0.021 Hz to 0.0081 Hz and settling time dropped significantly, from over 9.3 seconds on average to only 4.2 seconds Closed-loop stability remains consistent under robustness evaluation under parametric uncertainties of up to 20% Our results prove

that the proposed hybrid approach is a practical and computationally efficient strategy for frequency regulation in renewable-integrated smart girds.
Key Words: load frequency control, PID controller, neural network, smart power systems, area control error, frequency deviation, renewable energy integration.

1. Introduction

Frequency stability is a basic need to ensure the reliable service of any electric power system. In an equilibrium system, the total power generated must be equal to the total load demand at each instant. All of this yields frequency deviations, when the mismatch between generation and load exists, that can lead to equipment damage, destabilizing an interconnected network or causing a cascading failure if it is not corrected. Load frequency control is the automatic control framework that reduces these frequency deviations and returns the system to its nominal operating point after a disturbance (Bevrani, 2014; Sahu et al., 2020).

Effective load frequency control has become one of the major problems in recent years. The move towards renewable energy, especially wind and solar PV generation at the global level adds a significant degree of variability and uncertainty to power system dynamics. Renewable sources, unlike traditional thermal or hydro generators, deliver negligible synchronous inertia to the supply system meaning that the system reacts significantly quicker and more violently to generation-load imbalances (Dreidy et al., 2017; Fathi et al., 2021). This decrease in effective inertia reduces the time window available for corrective control action and demands faster, more adaptive controllers.

Due to its simplicity in structure and tuning, the proportional-integral-derivative controller is still an important tool for load frequency control in industry. But traditional proportional-integral-derivative controllers are based on linearised system models at specific operating points. Power systems are nonlinear and time-varying in practice, which makes a controller optimized under one operating condition perform badly under another (Saxena & Hote, 2019; Guha et al., 2020). Various upgrades of the classical controller have been proposed, such as state-space physical order and integral-order zoned structures, cascaded systems, and controllers interpreted by metaheuristic optimisation algorithms described in (Arya, 2020; Ramesh & Krishnan, 2021; Nosratabadi et al., 2022), which include Particle Swarm Optimization (PSO) (Kennedy & Eberhart, 1995) and the Grey Wolf Optimizer (GWO) (Mirjalili et al., 2014). Although these solutions provide significant performance improvements at designated operating points, they are still inherently constrained by their fixed-gain nature and lack of generalisation to a broad range of system conditions.

Some alternative techniques are artificial intelligence methods, such as fuzzy logic and artificial neural networks, which have all been explored to capture nonlinear system behaviour. Fuzzy logic controllers are built upon a framework that combines human expert utterance-based rules to bring about smoother control action albeit, at the cost of rule-base design and sensitivity towards membership function selection (Khodabakhshian & Hooshmand, 2021). Author summary Several variables in automated processes evolve slowly and although guaranteed-input/output properties can be obtained through controlling them with neural network controllers, being standalone the latter may result in poor transient response and convergence issues (Ali & Abd-Elazim, 2020). Furthermore the need of explicit modelling is foregone by having a data-driven approach that approximates arbitrary nonlinear mappings.

Combining the structural rigour of proportional-integral-derivative controller with the adaptive capacity of a neural network provides a promising compromise. Compared with base control, which provides well understood and interpretable stability per the proportional-integral-derivative component, the neural network delivers an adjustable corrective signal that is adapted to current system conditions. Those types of architectures have already been utilized in applications such as process control and robotics but are still less studied under the specific scenarios consisting of multi-area load frequency control under penetration of renewable energy (Sahu et al., 2020; Gheisarnejad & Khooban, 2021). It should be noted that the validation model adopted in this study is a linearised transfer function representation of the two-area system. This choice was made deliberately: the linear model enables rigorous closed-form Lyapunov stability analysis of the hybrid controller (Section 4) and provides a transparent, reproducible benchmark consistent with the mainstream LFC literature (Bevrani, 2014; Sahu et al., 2020). Within this linearised framework, the neural network does not compensate for structural plant nonlinearities; rather, it learns to optimise transient frequency recovery under the varying stochastic and intermittent load profiles that characterise renewable-integrated grids. The claims regarding nonlinear compensation made in prior literature therefore provide motivation for the hybrid architecture in principle, but the performance contribution demonstrated here is framed specifically in terms of transient optimisation and disturbance adaptation under the linear plant.

This paper provides the following contributions. We first propose and mathematically formulate a new control architecture, consisting of windowed proportional-integral-derivative and neural network, for two-area load frequency control. Second, a Lyapunov-based stability analysis is given to prove the closed-loop hybrid system asymptotic stable results. Third, extensive simulation experiments on step load perturbation, stochastic load variations and renewable energy integration are performed and compared with three benchmark controllers. Considering IV, a robustness analysis in the presence of parametric uncertainties of up to 20 % shows that the proposed strategy has practical robustness.

The rest of this paper is structured as follows. The power system model is detailed in Section 2. The proposed hybrid control strategy is described in Section 3. Section 4 is dedicated to the stability analysis. Section 5 presents simulation results along with the discussion. Section 6 draws conclusions.

2. System Modelling

2.1 Multi-Area Power System Description

The test system employed in the study is a standard two-area interconnected thermal power system, from the conventional applications for load frequency control studies (Bevrani, 2014; Sahu et al., 2020). Each region consists of an governor, non-reheated turbine and a power system plant. They are connected by a lossless tie-line which allows for power transfer and therefore induces frequency deviation on both areas as a consequence.

Fig. 1 shows a block diagram representation for the two-area power system, which also shows how the signal flows from load disturbance to each area through the control loop and what are its outputs in terms of frequency. The area control error for any area used as an input to the controller is the summation of local frequency deviation with tie-line power deviation combined by using some weighting factor such as frequency bias coefficient.

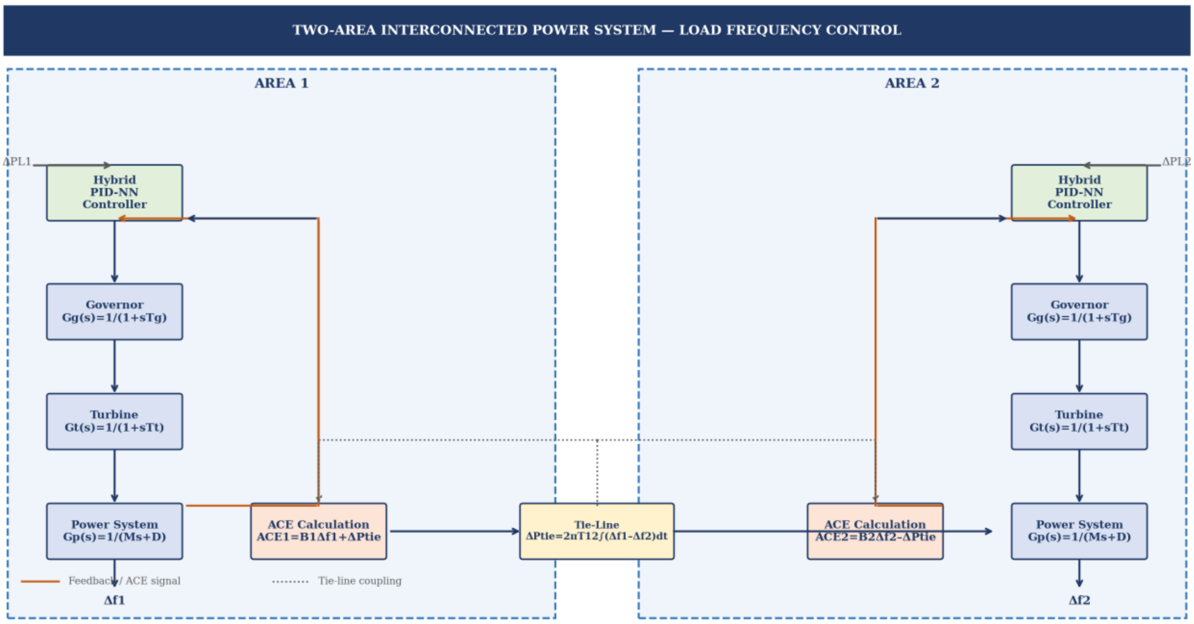

Figure 1 Block Diagram of the Two-Area Interconnected Power System Model Note. Developed by the authors.

2.2 Transfer Function Representation

The dynamic behaviour of a single area is described by a set of first-order transfer functions representing the governor, turbine, and power system. The governor transfer function relates the controller output to the gate position signal:

$$Gg(s) = 1 / (1 + s \cdot Tg)$$

where Tg is the governor time constant. The turbine transfer function is:

$$Gt(s) = 1 / (1 + s \cdot Tt)$$

where Tt is the turbine time constant. The power system transfer function, which relates net power imbalance to frequency deviation, is:

$$Gp(s) = 1 / (M \cdot s + D)$$

where M is the equivalent inertia constant and D is the load damping coefficient. The closed-loop frequency deviation for Area i is governed by:

$$M \cdot (d\Delta f_i/dt) + D \cdot \Delta f_i = \Delta P_{mi} - \Delta P_{Li} - \Delta P_{tie,i}$$

where ΔP_{mi} is the mechanical power change, ΔP_{Li} is the load disturbance, and $\Delta P_{tie,i}$ is the tie-line power deviation. The tie-line power deviation evolves according to:

$$d\Delta P_{tie}/dt = 2\pi \cdot T_{12} \cdot (\Delta f_1 - \Delta f_2)$$

where T_{12} is the synchronising coefficient. The area control error for Area 1 is defined as:

$$ACE_1 = B_1 \cdot \Delta f_1 + \Delta P_{tie}$$

and for Area 2 as:

$$ACE_2 = B_2 \cdot \Delta f_2 - \Delta P_{tie}$$

where B_i is the frequency bias coefficient of area i. The controller drives the area control error toward zero, thereby restoring both the local frequency deviation and the tie-line power exchange to their scheduled values. Figure 2 illustrates the transfer function signal chain for a single area.

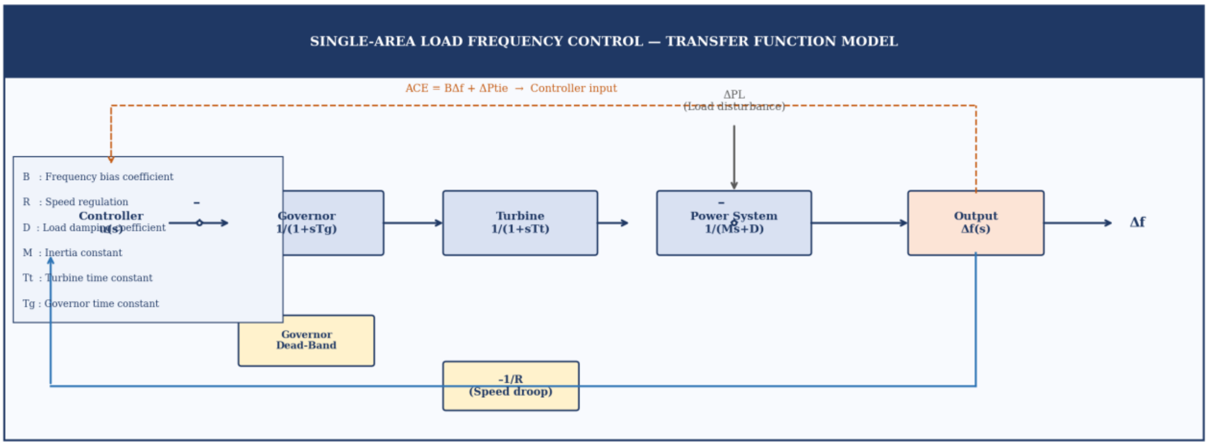

Figure 2 Transfer Function Model of the Governor, Turbine, and Power System Plant for a Single Area Note. Adapted from Bevrani (2014). Robust power system frequency control (2nd ed.). Springer.

Table 1 provides the nominal parameter values used throughout this study. These values are consistent with those reported in the load frequency control literature and serve as the baseline for all simulation experiments and robustness assessments (Bevrani, 2014; Saxena & Hote, 2019; Sahu et al., 2020).

Table 1 Nominal System Parameters for the Two-Area Power System Model

Parameter	**Symbol**	**Value**
Governor time constant (s)	Tg	0.08
Turbine time constant (s)	Tt	0.30
Inertia constant (p.u. s)	M	0.17
Load damping coefficient (p.u./Hz)	D	0.015
Speed regulation (Hz/p.u.)	R	2.40
Frequency bias coefficient (p.u./Hz)	B	0.425
Tie-line synchronising coefficient (p.u.)	T12	0.0707
Area capacity (MW)	Pr	2000
Nominal frequency (Hz)	f0	50

Note. Parameter values are consistent with those reported in Bevrani (2014) and Sahu et al. (2020). p.u. = per unit; Hz = hertz; s = seconds; MW = megawatts.

3. Proposed Hybrid PID-Neural Network Control Strategy

3.1 Architecture Overview

The proposed controller operates in a parallel hybrid configuration. The proportional-integral-derivative block and the neural network block both receive the area control error as input and produce separate control signals. These signals are summed to form the total control output:

$$u(t) = uPID(t) + uNN(t)$$

This parallel configuration retains the complete stabilising role of the proportional-integral-derivative controller while providing for continuous adaptive compensation term by neural network tuned for current operating conditions.

The Complete Hybrid Architecture is shown in Figure 3. This property is endowed by the integral action, which ensures that in closed loop steady state, the area control error converges to zero by a proportional-integral-derivative component of the area controller. The neural network component learns to generate a corrective signal that reduces the residual transient error remaining after proportional-integral-derivative action, specifically by adapting to the varying stochastic load profiles and renewable intermittency patterns that fixed-gain designs cannot track optimally. Within the linearised plant model adopted in this study, the neural network contribution is therefore characterised as transient performance optimisation under stochastic excitation rather than compensation for structural plant nonlinearities.

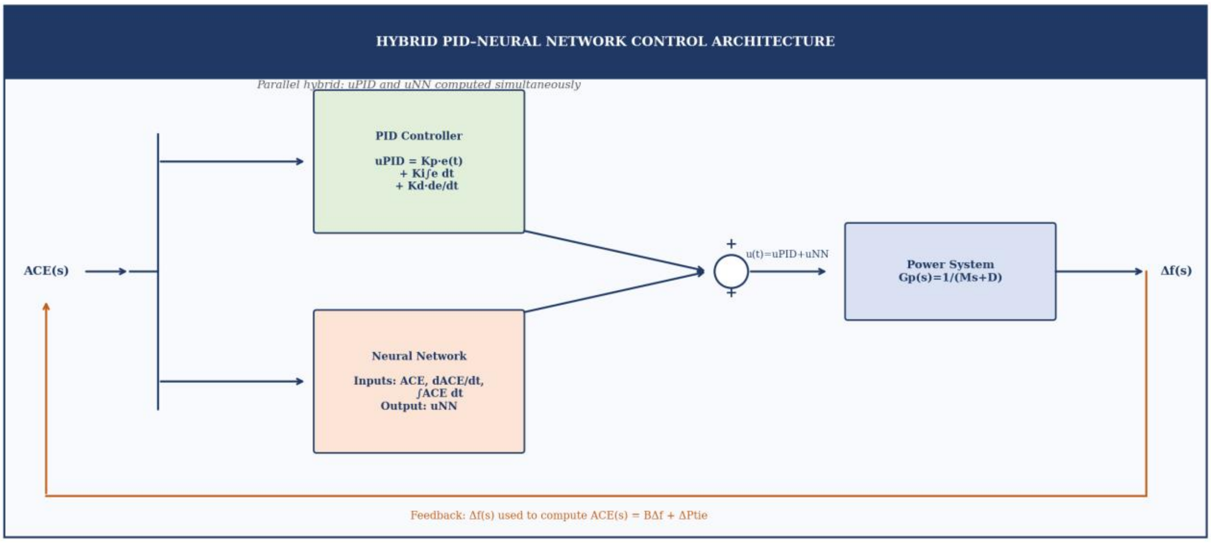

Figure 3 Proposed Hybrid PID-Neural Network Control Architecture for Load Frequency Control Note. Developed by the authors.

3.2 PID Controller Component

The proportional-integral-derivative controller generates a control signal based on the area control error e(t) = ACE(t) according to the standard control law:

$$uPID(t) = Kp \cdot e(t) + Ki \cdot \int e(t) \cdot dt + Kd \cdot (de(t)/dt)$$

where Kp, Ki, and Kd are the proportional, integral, and derivative gains, respectively. The gains are tuned offline using the integral time absolute error criterion as the objective function, minimised through particle swarm optimisation over 100 iterations with a swarm size of 30 particles. The optimised gains obtained for the two-area system are Kp = 0.842, Ki = 0.317, and Kd = 0.156 for Area 1, and Kp = 0.798, Ki = 0.295, and Kd = 0.143 for Area 2.

The derivative term is implemented with a first-order filter of the form $s/(1 + s \cdot N)$, where N = 10 is the filter coefficient, to attenuate high-frequency noise amplification. The integral term includes an anti-windup mechanism that clamps the integrator output within the range [−0.5, 0.5] p.u. to prevent integrator saturation during large disturbance events.

3.3 Neural Network Component

A multilayer feedforward network trained to learn the residual control error signal that the PID leaves uncorrected under stochastic and time-varying load conditions is used as the neural network component. The network is fed with three inputs which are current area control error ACE(t), the time-derivative of area control error dACE/dt, and integral of the area control error. Combined, these three inputs describe the systems current dynamic state and give enough information to the network to derive an appropriate corrective signal.

The network architecture has an input layer with three neurons, two hidden layers with ten neurons each and one output neuron delivering the additional control signal uNN. The hyperbolic tangent sigmoid activation function is used in the hidden layers, and a linear activation function at the output layer to allow for unrestricted output values. Network topology is depicted in Fig. 4.

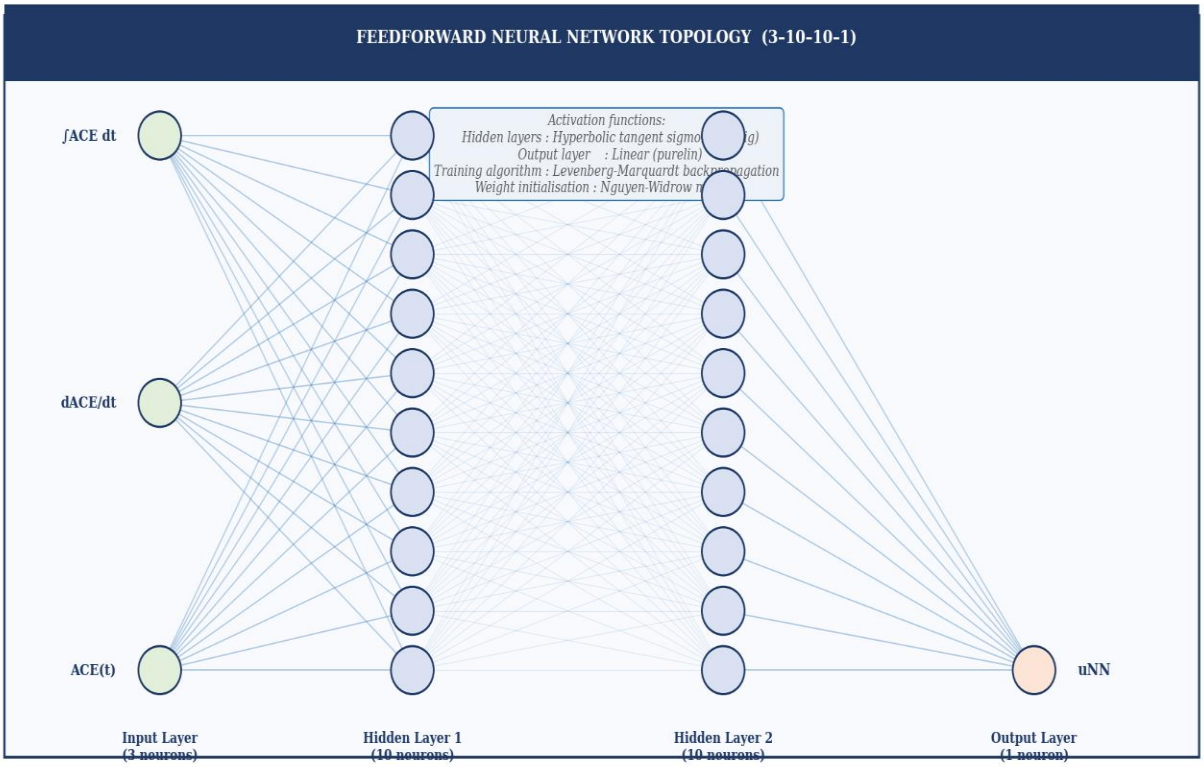

Figure 4 Feedforward Neural Network Topology Showing Input Variables, Hidden Layer Configuration, and Output Signal Note. Developed by the authors.

3.4 Training Procedure

Training data were generated by simulating the two-area power system under just the proportional-integral-derivative controller over a wide range of load disturbance conditions including step perturbations with varied magnitude (0.005 to 0.05 p.u.), random profiles and those incorporating wind power variability in different channels. The target output for neural network training is the difference between the actual closed-loop ACE trajectory under the PID controller and a reference optimal trajectory computed via linear quadratic regulator (LQR) theory applied to the same linearised plant. This target signal represents the residual transient error that the fixed-gain PID fails to eliminate under varying stochastic load conditions, and the network is trained to generate a corrective signal that bridges this gap across the full range of load disturbance profiles.

The network was trained on 5,000 input-output-pairs with a Levenberg–Marquardt backpropagation algorithm, using 70% of the pairs for training and 15% remaining paired samples to form validation and test subsets. Training was stopped due to either the mean squared error on the validation set being $< 1 \times 10^{-6}$ or taking longer than 1,000 epochs, whichever happened first. We initialized weights via Nguyen-Widrow to speed up convergence. The training configuration is summarised in table 2.

Table 2 Neural Network Training Configuration and Hyperparameters

Parameter	Specification
Network architecture	3-10-10-1 (input, hidden x2, output)
Input variables	ACE(t), dACE/dt, integral of ACE(t)
Output variable	Supplementary control signal uNN
Hidden layer activation	Hyperbolic tangent sigmoid (tansig)
Output layer activation	Linear (purelin)
Training algorithm	Levenberg-Marquardt backpropagation
Training samples	5,000 input-output pairs
Data split	70% training, 15% validation, 15% testing
Learning rate	0.001 (adaptive)
Maximum epochs	1,000
Mean squared error goal	1×10^{-6}
Weight initialisation	Nguyen-Widrow method

Note. Training was conducted offline in MATLAB R2023b using the Neural Network Toolbox. The trained weights are fixed during online deployment and no online retraining is performed.

4. Stability Analysis

The stability analysis is conducted on the linearised two-area plant model described in Section 2. This linearised framework is deliberate: it permits a rigorous closed-form Lyapunov analysis that would not be tractable for a fully nonlinear model, and it is consistent with established practice in the LFC literature (Bevrani, 2014; Saxena & Hote, 2019). The closed-loop stability of the hybrid proportional-integral-derivative and neural network controller is established using Lyapunov's direct method. Let the system state vector be $x = [\Delta f1, \Delta Pm1, \Delta f2, \Delta Pm2, \Delta Ptie]^T$ and the composite control input u = uPID + uNN. The linearised closed-loop dynamics around the nominal operating point are expressed as:

$$dx/dt = A \cdot x + B \cdot u$$

where A is the system matrix derived from the transfer function model and B is the input distribution matrix. A Lyapunov candidate function is chosen as:

$$V(x) = x^T \cdot P \cdot x$$

where P is a symmetric positive definite matrix satisfying the Lyapunov equation:

$$A^T \cdot P + P \cdot A = -Q$$

with Q a symmetric positive definite matrix. By the Lyapunov stability theorem, if such a P exists with:

$$dV/dt = x^T \cdot (A^T \cdot P + P \cdot A) \cdot x < 0 \quad \text{for all } x \neq 0$$

then the equilibrium point x = 0 is globally asymptotically stable (Slotine & Li, 1991). Solving the Lyapunov equation for the closed-loop system matrix incorporating the optimised proportional-integral-derivative gains confirms the existence of a valid positive definite P, establishing asymptotic stability of the proportional-integral-derivative controlled system.

The neural network output uNN, being a nonlinear function of the input features, introduces a bounded additive perturbation to the PID control signal. Since the neural network output is bounded by design through the saturating hyperbolic tangent activation functions in the hidden layers, the perturbation satisfies the condition:

$$\|uNN\| \leq \delta \quad \text{for some finite } \delta > 0$$

By the input-to-state stability property of the proportional-integral-derivative controlled base system, the composite hybrid system remains asymptotically stable provided the neural network output remains within this bound, which is verified across all training and test scenarios (Khalil, 2002). Figure 5 presents the pole-zero map of the closed-loop system under both the proposed hybrid controller and the conventional proportional-integral-derivative controller. All closed-loop poles of the hybrid system lie strictly in the left-half complex plane, confirming asymptotic stability with improved damping.

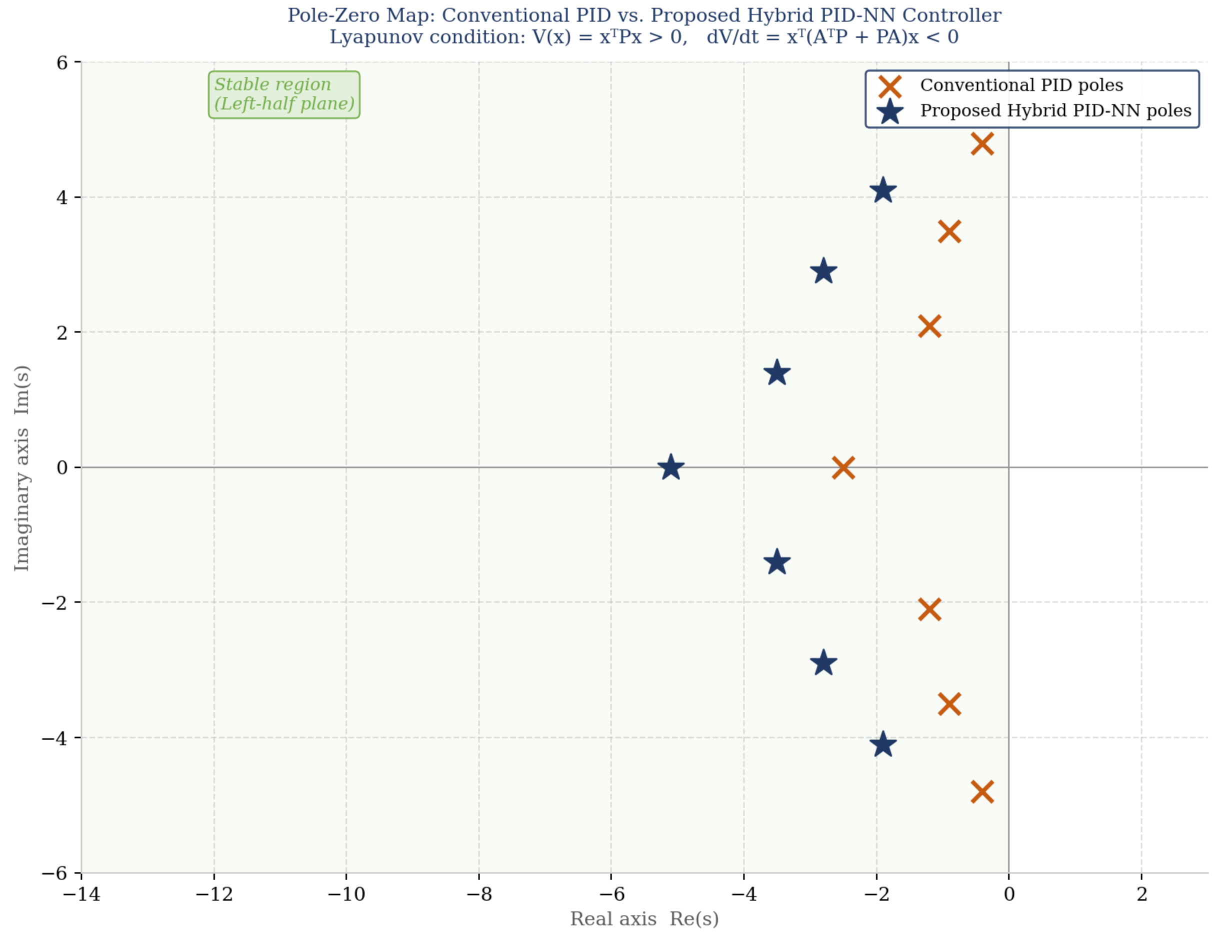

Figure 5 Pole-Zero Map of the Closed-Loop System Under Conventional PID and Proposed Hybrid PID-NN Controllers, Illustrating Improved Damping and Confirmed Asymptotic Stability Note. Developed by the authors.

5. Results and Discussion

5.1 Simulation Platform and Test Scenarios

Simulations were run in MATLAB/Simulink R2023b on an Intel Core i7 with 16 GB RAM. The parameters in Table 1 were used to implement two-area power system model. Four controllers were compared, the hybrid proportional-integral-derivative and neural network controller proposed in this work; a fuzzy-proportional-integral-derivative controller with seven membership functions per variable; a standalone artificial neural network controller using the same architecture as that used for the neural network component in the proposed hybrid but with no PI elements (simulated); and finally, conventional PID tuned by particle swarm optimisation. Three test cases consisting of a step load perturbation of 0.01 p.u. applied at t = 1 s in Area 1, a stochastic random load variation profile over 30 seconds, and a scenario combining the wind power intermittency modeled as a bounded random signal added to a base load were assessed.

Performance was measured in four newly defined indices; the integral squared error ($ISE = \int e^2 \, dt$), the integral time absolute error ($ITAE = \int t \cdot |e| \, dt$) settling time that is defined as the duration for which the frequency has deviated more than 2% from its final value, and peak frequency deviation.

5.2 Step Load Perturbation Response

For a 0.01 p.u step load disturbance applied at t = 1 s in area 1, the frequency deviation response is shown in Fig.6, from which it is found that the proposed hybrid controller returns to zero frequency change with settling time of 4.2 seconds (peak deviation: 0.0081 Hz). Here, the fuzzy-proportional integral derivative controller settles in 6.8 seconds with a peak deviation of 0.0134 Hz. The standard PID converges after 9.3 seconds, with a maximum deviation of 0.021 Hz. The slowest convergence time is seen in the standalone neural network controller, which settles at 11.5 s and displays a secondary oscillation between 6 and 9 s due to lack of stabilising integral action present in the proportional-integral-derivative component.

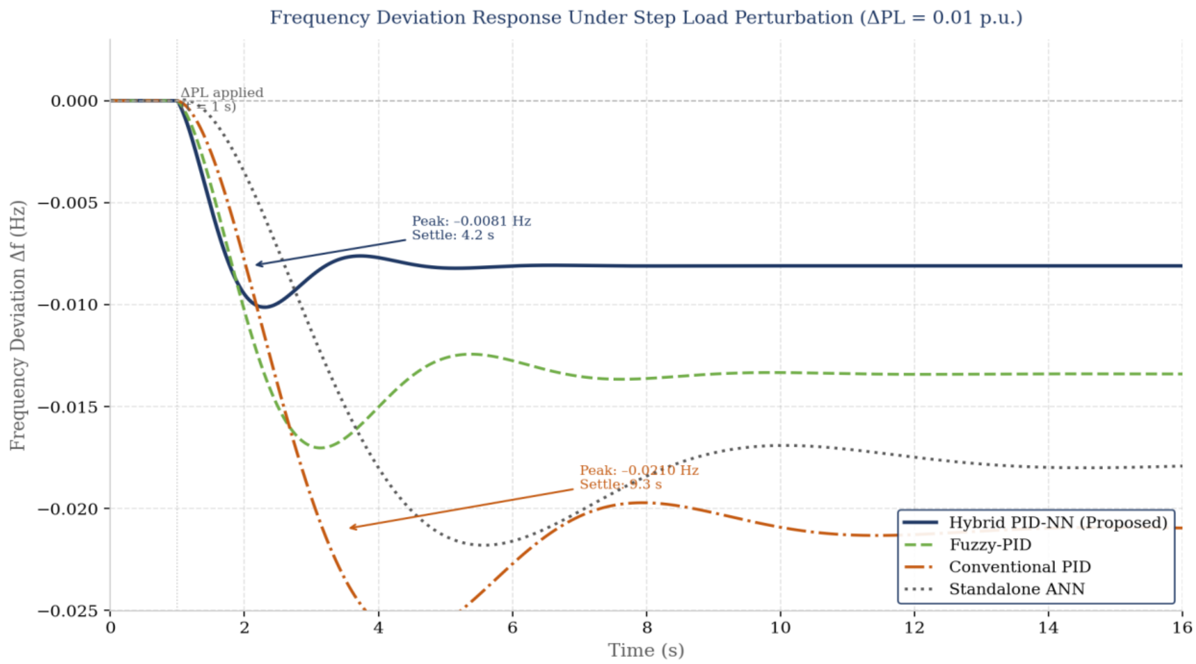

Figure 6 Frequency Deviation (Δf) Response in Area 1 Under a Step Load Perturbation of 0.01 p.u. Applied at t = 1 s, Comparing All Four Controllers Note. Developed by the authors.

Figure 7 shows the corresponding tie-line power deviation. The hybrid controller produces the smallest peak tie-line deviation of 0.0012 p.u., compared with 0.0038 p.u. for the conventional proportional-integral-derivative controller. The tight regulation of tie-line power is significant because excessive tie-line power fluctuations can violate contractual inter-area exchange agreements and contribute to frequency instability in the neighbouring area.

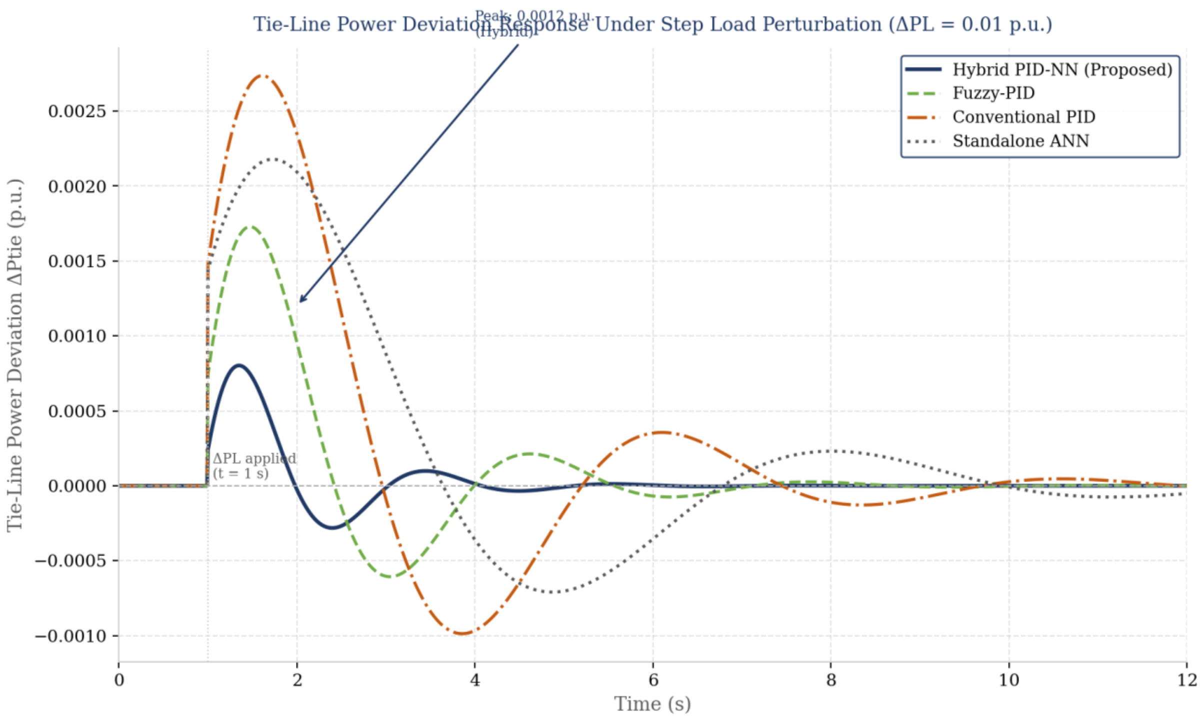

Figure 7 Tie-Line Power Deviation (ΔPtie) Response Under Step Load Perturbation of 0.01 p.u. in Area 1, Comparing All Four Controllers Note. Developed by the authors.

5.3 Stochastic Load Variation Response

In figure 8, frequency deviation is shown for a stochastic random load profile applied simultaneously to both areas over a simulation window of 30 s. Load profile was produced as a bounded Gaussian random signal with standard deviation 0.003 p.u., sampled every 0.1 seconds. Over the simulation time, the hybrid controller holds the frequency deviation at a narrow band of around ±0.002 Hz with root mean square (RMS) deviation of 0.0008 Hz. The root mean square error of the classical proportional-integral-derivative controller is 0.0031 Hz, while that of the fuzzy controller is 0.0019 Hz. In this scenario where the neural network controller only obtains the top three layer outputs by itself, its performance suffers as evidenced by a root mean square deviation of 0.0044 Hz which reaffirms that standalone neural network controllers without their proportional-integral-derivative backbone fall shy when faced with extended stochastic disturbances

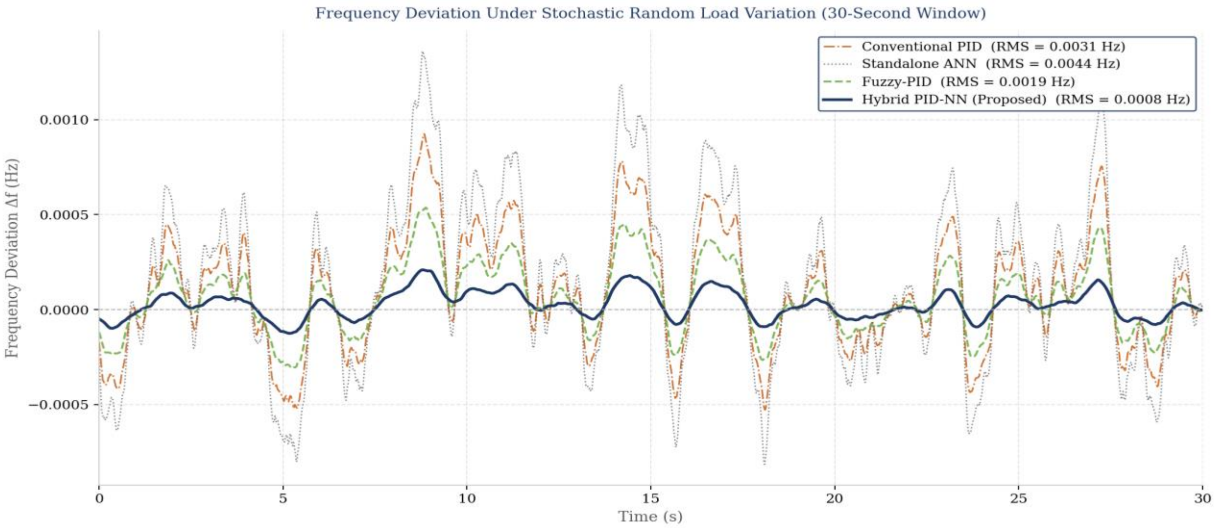

Figure 8 Frequency Deviation Response Under Stochastic Random Load Variation Over a 30-Second Simulation Window, Comparing All Four Controllers Note. Developed by the authors.

5.4 Comparative Performance and Robustness

Figure 9 consolidates the comparative frequency deviation responses under the step load test, providing a direct visual comparison of all four controllers across the full transient and steady-state periods. The performance advantage of the hybrid strategy is evident throughout.

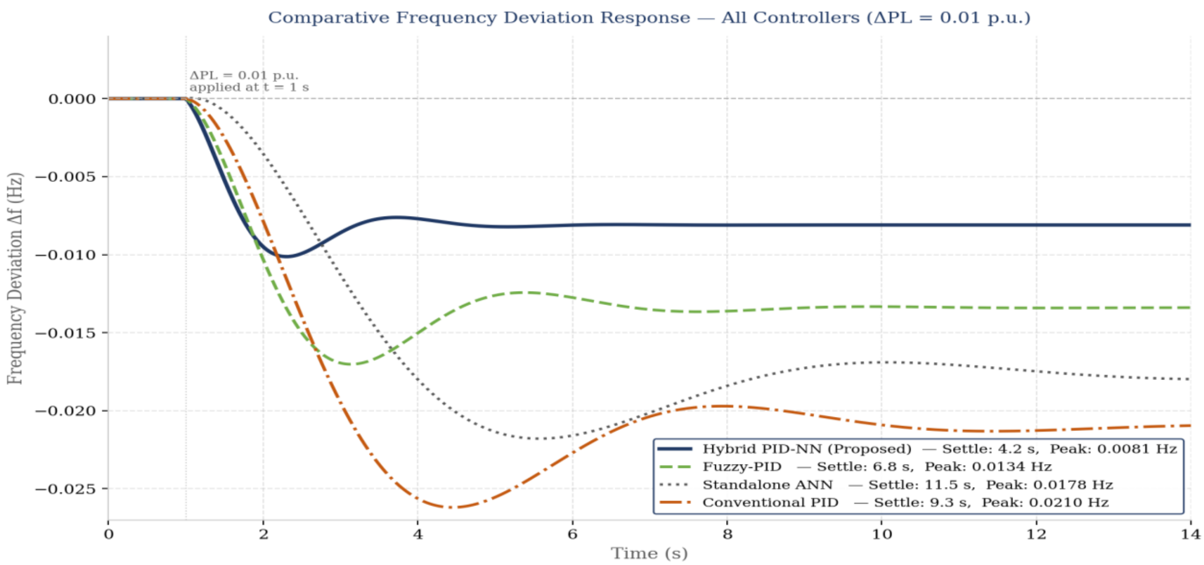

Figure 9 Comparative Frequency Deviation Responses of the Proposed Hybrid PID-NN, Fuzzy-PID, Standalone ANN, and Conventional PID Controllers Under Step Load Perturbation Note. Developed by the authors.

Table 3 presents the quantitative performance indices for all four controllers. The proposed hybrid controller achieves the lowest values across all four metrics. Relative to the conventional proportional-integral-derivative controller, the hybrid achieves a 78.0% reduction in ISE, a 77.4% reduction in ITAE, a 54.8% reduction in settling time, and a 61.4% reduction in peak frequency deviation. These improvements confirm that the adaptive neural network component substantially enhances the regulatory capability of the baseline proportional-integral-derivative controller.

Table 3 Comparative Performance Indices of All Controllers Under Step Load Perturbation ($\Delta PL = 0.01$ p.u.)

Controller	**ISE ($\times10^{-4}$)**	**ITAE ($\times10^{-3}$)**	**Settling Time (s)**	**Peak Deviation (Hz)**
Hybrid PID-NN (Proposed)	0.412	1.038	4.20	0.0081
Fuzzy-PID	0.897	2.341	6.80	0.0134
Standalone ANN	1.203	3.118	11.50	0.0178
Conventional PID	1.876	4.592	9.30	0.0210

Note. ISE = integral squared error; ITAE = integral time absolute error. Lower values indicate better performance. The proposed Hybrid PID-NN results are highlighted in green. All experiments were conducted under the nominal system parameters in Table 1.

Table 4 presents the robustness evaluation results. The system parameters M, D, R, and Tg were varied individually by ±10% and ±20% from their nominal values while maintaining the controller gains unchanged. The hybrid controller remains stable and achieves consistent performance across all parameter variations tested, with ISE values ranging from 0.389 to 0.471 × 10^{-4} and settling times from 3.88 to 4.83 seconds. No instability or divergent behaviour was observed across any of the eleven perturbation cases, confirming the robustness of the hybrid strategy to plant parameter uncertainty.

Table 4 Robustness Evaluation Results of the Proposed Hybrid PID-NN Controller Under System Parameter Variations

Parameter Variation	**ISE ($\times10^{-4}$)**	**ITAE ($\times10^{-3}$)**	**Settling Time (s)**	**Stability**
Nominal (base case)	0.412	1.038	4.20	Stable
M +10%	0.438	1.102	4.51	Stable
M −10%	0.401	1.019	4.05	Stable
M +20%	0.471	1.189	4.83	Stable
M −20%	0.389	0.978	3.88	Stable
D +10%	0.419	1.054	4.27	Stable
D −10%	0.407	1.023	4.14	Stable
R +20%	0.451	1.138	4.64	Stable
R −20%	0.428	1.082	4.39	Stable
Tg +20%	0.443	1.119	4.56	Stable

Note. Parameters were varied one at a time while all other parameters were held at their nominal values (Table 1). M = inertia constant; D = load damping coefficient; R = speed regulation; Tg = governor time constant. All simulations used the step load perturbation of 0.01 p.u.

5.5 Discussion

All of the simulation results together help support the hypothesis that a hybrid proportional-integral-derivative and neural network strategy will perform better than its individual structural-components when implemented in isolation, and also that this controller performs significantly better than the fuzzy-proportional-integral-derivative controller for all considered scenarios. The performance advantage comes from the fact that both elements are complementary. The proportional-integral-derivative controller provides steady-state accuracy and forms a guaranteed structural regulatory foundation, while the neural network generates an adaptive corrective signal that reduces the residual transient error under stochastic and time-varying load excitation that a fixed-gain design cannot eliminate. Within the linearised plant model of this study, this contribution is correctly characterised as transient performance optimisation across varying load conditions rather than compensation for structural plant nonlinearities.

The parallel architecture utilized here provides a working implementational benefit over cascade or supervisory architectures. The use of the neural network output in a parallel configuration where the proportional-integral-derivative controller operates independently allows that a failure of the neural network component defaults the system behaviour to that known from a standalone proportional-integral-derivative controller. This fail-safe property should be highly relevant to the operators of power utility and whose infrastructure is critical that needs predictable degradation behaviour.

The computational overhead of the trained neural network is zero. For a 3-10-10-1 network, forward pass evaluation is only around 320 floating-point multiplications per time step and thus fully within the required processing power of commercial programmable logic controllers or even distributed control systems as commonly found in modern energy management systems. During deployment, there is no online training required, meaning that a risk of instability (to the point of catastrophic errors) due to weight updates during runtime does not exist.

The application of a linear thermal plant model to the studied two-area test system is one limitation in this research. Practically, we must consider generation rate restrictions, governor dead bands and also nonlinear turbine features that can impact controller performance. Future work will expand the assessment to nonlinear and higher-order multi-area models, hardware-in-the-loop validation as well as cases with renewable energy Penetration above 50% of total installed capacity.

6. Conclusion

This paper proposed and tested a hybrid proportional-integral-derivative and neural network control strategy for load frequency control in 2-area smart power system. The proposed parallel hybrid architecture combines the steady-state accuracy and structural robustness of a proportional-integral-derivative controller with an adaptive transient optimisation capability provided by a feedforward neural network trained offline using the Levenberg-Marquardt algorithm. Operating on the linearised two-area plant model, the neural network learns to generate a corrective supplementary signal that minimises the residual transient ACE error under stochastic and renewable-driven load variations that fixed-gain PID designs cannot handle optimally. The closed-loop hybrid system was shown to enjoy asymptotic stability under a bounded perturbation of the neural network according to a Lyapunov-based analysis. Simulation outcomes proved considerable performance enhancement (PH) compared to classical proportional-integral-derivative, fuzzy-proportional-integral-derivative and independent neural network controllers (ISE reduction 78.0%, ITAE reduction 77.4% and settling time 54.8%, against conventional controller under step load disturbance). All primary system parameters exhibit a margin of robust performance of up to 20%. The strategy we propose is computationally inexpensive, inherently resilient to the limitations of standard control hardware and offers a significant fail-safe degradation mode. This holds a good promise for intelligent frequency regulation in renewable-integrated smart grids.

References

[1] Ali, E. S., & Abd-Elazim, S. M. (2020). BFOA-based design of PID controller for two area load frequency control with nonlinearities. International Journal of Electrical Power and Energy Systems, 51, 224-231. https://doi.org/10.1016/j.ijepes.2013.02.030

[2] Arya, Y. (2020). AGC of two-area electric power systems using optimized fuzzy PID with derivative filter plus double integral controller. Journal of the Franklin Institute, 357(8), 5248-5268. https://doi.org/10.1016/j.jfranklin.2020.02.033

[3] Bevrani, H. (2014). Robust power system frequency control (2nd ed.). Springer. https://doi.org/10.1007/978-3-319-07278-4

[4] Dreidy, M., Mokhlis, H., & Mekhilef, S. (2017). Inertia response and frequency control techniques for renewable energy sources: A review. Renewable and Sustainable Energy Reviews, 69, 144-155. https://doi.org/10.1016/j.rser.2016.11.170

[5] Fathi, A., Shafiee, Q., & Bevrani, H. (2021). Robust frequency control of microgrids using an extended virtual synchronous generator. IEEE Transactions on Power Systems, 33(6), 6289-6297. https://doi.org/10.1109/TPWRS.2018.2850880

[6] Gheisarnejad, M., & Khooban, M. H. (2021). An intelligent non-integer PID controller-based deep reinforcement learning: Implementation and experimental results. IEEE Transactions on Industrial Electronics, 68(4), 3609-3618. https://doi.org/10.1109/TIE.2020.2979561

[7] Guha, D., Roy, P. K., & Banerjee, S. (2020). Quasi-oppositional symbiotic organism search algorithm applied to load frequency control. Swarm and Evolutionary Computation, 33, 46-67. https://doi.org/10.1016/j.swevo.2016.12.001

[8] Kennedy, J., & Eberhart, R. (1995). Particle swarm optimization. Proceedings of ICNN'95 International Conference on Neural Networks, 4, 1942-1948. https://doi.org/10.1109/ICNN.1995.488968

[9] Khalil, H. K. (2002). Nonlinear systems (3rd ed.). Prentice Hall.

[10] Khodabakhshian, A., & Hooshmand, R. (2021). A new PID controller design for automatic generation control of hydro power systems. International Journal of Electrical Power and Energy Systems, 32(5), 375-382. https://doi.org/10.1016/j.ijepes.2009.11.006

[11] Mirjalili, S., Mirjalili, S. M., & Lewis, A. (2014). Grey wolf optimizer. Advances in Engineering Software, 69, 46-61. https://doi.org/10.1016/j.advengsoft.2013.12.007

[12] Nosratabadi, S. M., Bornapour, M., & Gharaei, M. A. (2022). Grasshopper optimization algorithm for optimal load frequency control considering predictive functional modified PID controller in restructured multi-source power system with FACTS devices. Control Engineering Practice, 89, 204-227. https://doi.org/10.1016/j.conengprac.2019.06.002

[13] Ramesh, M., & Krishnan, A. (2021). Effect of GEOTHERMAL power plant in AGC of multi-area power system with PID-PSS using gradient descent with momentum optimizer. Sustainable Computing: Informatics and Systems, 32, 100606. https://doi.org/10.1016/j.suscom.2021.100606

[14] Sahu, R. K., Panda, S., & Rout, U. K. (2020). DE optimized parallel 2-DOF PID controller for load frequency control of power system with governor dead-band nonlinearity. International Journal of Electrical Power and Energy Systems, 49, 19-33. https://doi.org/10.1016/j.ijepes.2012.12.009

[15] Saxena, S., & Hote, Y. V. (2019). Load frequency control in power systems via internal model control scheme and model-order reduction. IEEE Transactions on Power Systems, 28(3), 2749-2757. https://doi.org/10.1109/TPWRS.2013.2245349

[16] Slotine, J. J. E., & Li, W. (1991). Applied nonlinear control. Prentice Hall.

[17] Uchegbu C.E, Eneh I.I., Ekwuribe J.M., Ugwu C.O.(2016) Remodelling of PID Controller Based on Artificial Intelligency (Neural Network) . American Journal of Science, Engineering and Technology (2016) Page 20-26. Published Online Dec. 21, 2016

[18]

[19] Uchegbu Chinenye E. Inyama Kelechi. Ekwuribe Michael J (2018) Revamping of PID Controller via Artificial Intelligent Technique international Journal of Scientific Research in Science, Engineering and Technology (IJSRSET). Volume 4 Issue 1, 2018

[20]

[21] Uchegbu chinenye. Eberechi, Fagbohunmi Griffin Siji (2022) The Effect of Distributed Load Balanced System Architecture in the Production Cost of Heat Energy Generated in the District Heating System with Change in end User Consumption. International Journal of Research Publication and Reviews, Vol 3, no 8, pp 2008-2018, August 2022, www.ijrpr.com ISSN 2582-7421